

Local and distributed voltage control algorithms in distribution network

Guido Cavraro, Ruggero Carli

Abstract—In this paper we consider a voltage control problem in power distribution grids. The specific goal is that of keeping the voltages within pre-assigned operating limits by commanding the reactive power output of the micro-generators connected to the grid. We propose three strategies. The first two strategies are purely local, meaning that each micro-generator updates the amount of reactive power to be injected based only on local measurements of the voltages' magnitude. Instead the third one is distributed, namely, the micro-generators, to perform the updating steps, require some additional information coming from the neighboring agents. The local strategies are simpler to be implemented but they might fail in solving the voltage control problem. Instead, the distributed one requires the micro-generators to be endowed with communication capabilities but it is effective in driving the voltages within the admissible intervals and, additionally, it exploits the cooperation among the agents to reach also a power losses minimization objective. Theoretical analysis and extensive numerical simulations are provided to confirm the arguments aforementioned.

I. INTRODUCTION

Recent technological advances, together with environmental and economic challenges, have been motivating the massive deployment of small power generators in the low voltage and medium voltage power distribution grid [1]. On one hand, significant benefits to the network operation could come from the availability of a large number of these generators in the distribution grid. They could provide a number of ancillary services, e.g., voltage profile improvements, reduction of line losses, reduction of power generation cost, just to mention a few [2], that are of great interest for the grid management. On the other hand, the uncontrolled injection of power from several renewable energy sources can cause serious system damages or system instabilities. For instance, operational bounds may be violated due to the intermittence of the renewable sources, as large voltages variations might occur. For these reasons, voltage regulation is a fundamental issue in the development of the future *smart distribution grid*.

In the past, electro-mechanical control devices, such as shunt capacitor banks or on-load tap changers [3], have been used to perform voltage control in distribution networks. However, they are typically too slow to properly respond to the voltage fluctuations due to the high variability of the load demand and of the energy resources, while inverters can act on a fast timescale in the grid. This has motivated the recent increasing interest for strategies that regulate the voltage magnitudes by directly actuating the injection (or absorption) of the micro-generators reactive power; indeed, when running below their rated output current, many inverters have the capability of

injecting (or of absorbing) reactive power together with active power [4].

The highly fluctuating behaviors of the renewable energy sources, call for *purely local* or *distributed* approaches to deal with the voltage regulation problem. *Purely local* means that agents use just local measurements and do not exchange information with each other; *distributed* means that agents, that are physically close, are allowed to communicate and can share information to cooperatively reach the pre-assigned objectives.

The purely local strategies (see [5], [6], [7], [8], [9], [10], [11]) typically aim to guarantee that voltage constraints are satisfied. Distributed strategies (see [12], [13], [14], [15]), beside local voltage constraints, take into account other important global objectives, e.g., power losses minimization, and drive the state system towards configurations which are obtained solving the so-called *optimal reactive power flow* (ORPF) problems. Strategies in [12], [13], [14] reformulate ORPF problems as a rank-constrained semidefinite programs, convexify them by eliminating the rank constraint and provide solutions in a distributed manner through standard optimization algorithms. However, these approaches require the monitoring of all the buses of the grid, which, in general, is not amenable of practical implementation in the distribution grid. This issue is overcome in [15] where not all the buses are required to be monitored. The algorithm proposed in [15] is based on the alternating actuation of the two following steps: gathering voltage measurements at the micro-generators buses and applying control laws based on these measured data.

Three voltage control strategies are proposed in this paper. The first two strategies (denoted as LVC-1 and LVC-2) are purely local. They are based on the classical droop controlled described in [4]. They exhibit a fast transient properties and are shown to converge to a steady state which, however, in general, is not guaranteed to meet the voltage constraints. At this regard, we provide a numerical example where for both LVC-1 and LVC-2, the micro-generators are not effective in regulating the voltage between the desired limits, even if the available reactive power resources would allow it, if properly dispatched. This issue is overcome by the third strategy (denoted as f-DORPF) which is a novel distributed algorithm improving the performance of the distributed strategy introduced in [15] (denoted as DORPF). Remarkably, in [15], it is shown that adding information exchanges between neighboring nodes allows the DORPF algorithm to solve the voltage control problem while also reaching a power losses minimization objective. However DORPF exhibits poor transient performance, namely, it requires a consistent number of iterations to approach the optimal solution. The main idea behind the f-DORPF algorithm we propose in this paper is that of combining the updating steps of DORPF with those of the purely local strategy LVC-2, thus obtaining fast transient properties and convergence to the same

G. Cavraro and R. Carli are with the Department of Information Engineering, University of Padova, Italy. Email: {cavraro, carlirug}@dei.unipd.it.

steady-state of the DORPF, i.e., the operating conditions are satisfied and the power losses are minimized.

The paper is organized as follows. A model of the distribution network is provided in Section III. In Section IV, we introduce the problem of regulating the voltages magnitudes through the reactive power injected by the micro-generators. In Section V and in Section VI, we illustrate, respectively, the two purely local strategies and the distributed strategy. Finally, we analyze and compare the performance of the various strategies in Section VII.

II. NOTATION AND MATHEMATICAL PRELIMINARIES

Let us denote by $\mathcal{G} = (\mathcal{V}, \mathcal{E})$ a undirected graph, where \mathcal{V} and \mathcal{E} denote, respectively, the set of nodes and the set of edges. Assume that $n = |\mathcal{V}|$ and $r = |\mathcal{E}|$. Given two nodes $h, k \in \mathcal{V}$, we define the path $\mathcal{P}_{hk} = (v_1, \dots, v_\ell)$ as the sequence of nodes, without repetitions, such that $v_1 = h$, $v_\ell = k$ and for each $i = 1, \dots, \ell - 1$, the nodes v_i and v_{i+1} are connected by an edge. Given a vector u , \bar{u} denotes its complex conjugate, while u^T denotes its transpose. Instead, $\Re(u)$ and $\Im(u)$ refer to its real and imaginary part (element-wise), respectively. Let the symbol $\mathbf{1}$ denote the column vector whose elements are all equal to one, while the symbol e_v denote the column vector whose elements are all equal to 0, except its v -th entry which is equal to 1. Given $w, \underline{w}, \bar{w} \in \mathbb{R}^\ell$, with $\underline{w}_h \leq \bar{w}_h, h = 1, \dots, \ell$, let the operator $[w]_{\underline{w}, \bar{w}}$ be the component-wise projection of u in the set $\{x \in \mathbb{R}^\ell : \underline{w}_h \leq x_h \leq \bar{w}_h, h = 1, \dots, \ell\}$, that is,

$$\left([w]_{\underline{w}, \bar{w}}\right)_h = \begin{cases} w_h & \text{if } \underline{w}_h \leq w_h \leq \bar{w}_h \\ \underline{w}_h & \text{if } w_h < \underline{w}_h \\ \bar{w}_h & \text{if } w_h > \bar{w}_h \end{cases} \quad (1)$$

Given a real number x we define the function $\text{sign}(x)$ as

$$\text{sign}(x) = \begin{cases} x/|x| & \text{if } x \neq 0 \\ 0 & \text{if } x = 0 \end{cases} \quad (2)$$

Given a matrix Λ , we denote with $\rho(\Lambda)$ its spectral radius, namely, the largest eigenvalue in absolute value.

III. SMART GRID CYBER-PHYSICAL MODEL

In this paper, we describe the *smart* power distribution network as a cyber-physical system, where the *physical layer* is composed by the power distribution infrastructure including the electric lines, micro-generators, loads and the point of connection to the transmission grid (denoted as PCC), while the *cyber layer* consists of the intelligent agents which are deployed in the electric grid.

A convenient way to model the physical layer is by a directed graph \mathcal{G} , where edges in \mathcal{E} represent the electric lines, and nodes in \mathcal{V} represent both loads and generators connected to the microgrid (see Figure 1). The following variables describe the overall state of the system:

- $u \in \mathbb{C}^n$, where u_h is the voltage at node h ;
- $v \in \mathbb{R}_{\geq 0}^n$, where v_h is the voltage magnitude at node h ;
- $i \in \mathbb{C}^n$, where i_h is the current that node h injects;
- $s = p + jq \in \mathbb{C}^n$, where s_h, p_h and q_h are the complex, the active and the reactive power injected at node h .

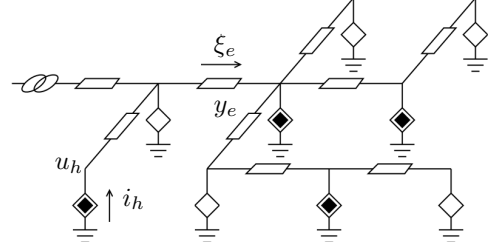


Figure 1. Circuitual representation of a microgrid, where black diamonds are micro-generators, white diamonds are loads, and the left-most element of the circuit represents the PCC.

We model the PCC as an ideal sinusoidal voltage generator (*slack bus*) at the grid nominal voltage U_N . Without loss of generality, we label the PCC as node 1 and we assume its voltage phase to be equal to 0. The powers s_h corresponding to grid loads are such that $p_h < 0$, which means that active power is *supplied* to the devices, while, when dealing with power micro-generators, we have that $p_h \geq 0$, which means that active power is *injected* into the grid. The system state satisfies the following relations

$$i = Y u, \quad u_1 = U_N, \quad (3)$$

$$u_h \bar{i}_h = p_h + jq_h \quad h \neq PCC, \quad (4)$$

where Y is the bus admittance matrix of the grid. The element Y_{hk} represents the admittance of the line connecting bus h with bus k . The Green matrix $X \in \mathbb{R}^{n \times n}$, which depends only on the topology of the grid power lines and on their impedances, is the unique symmetric positive semidefinite matrix, see [15], such that

$$u = X i + \mathbf{1} U_N. \quad (5)$$

In our setup, each micro-generator corresponds to an *agent* in the cyber layer and belongs to the set $\mathcal{C} \subseteq \mathcal{V}$ (with $|\mathcal{C}| = m$). We assume that the agents are provided with *sensing capabilities*, in particular *voltage phasor measurement units* (PMU) (devices that measure both magnitude and phase of the voltages) and with *computational capabilities* that will be exploited in the proposed algorithms implementation. In particular, the agents can regulate the amount of reactive power injected into the grid. To underline the difference among smart agents and passive loads, we adopt the following block decomposition of the voltage vector u

$$u = [u_1 \quad u_G^T \quad u_L^T], \quad (6)$$

where u_1 is the voltage at the PCC, $u_G \in \mathbb{C}^m$ are the voltages at the micro-generators, and $u_L \in \mathbb{C}^{n-m-1}$ are the voltages at the loads. Similarly, $s_G = p_G + jq_G$ and $s_L = p_L + jq_L$. Following the same partitioning, we can block-partition X as

$$X = \begin{bmatrix} 0 & 0 & 0 \\ 0 & M & N \\ 0 & N^T & Q \end{bmatrix},$$

where $M \in \mathbb{C}^{m \times m}, N \in \mathbb{C}^{m \times n-m-1}, Q \in \mathbb{C}^{n-m-1 \times n-m-1}$. The non-linear relation between u and s , can be conveniently

linearized as in [15], by

$$\begin{bmatrix} u_G \\ u_L \end{bmatrix} = \frac{1}{U_N} \begin{bmatrix} M & N \\ N^T & Q \end{bmatrix} \begin{bmatrix} \bar{s}_G \\ \bar{s}_L \end{bmatrix} + \mathbf{1}U_N. \quad (7)$$

Interestingly, equation (7) can be used to approximate the voltages magnitudes as

$$\begin{bmatrix} v_G \\ v_L \end{bmatrix} = \frac{1}{U_N} \Re \begin{bmatrix} M & N \\ N^T & Q \end{bmatrix} \begin{bmatrix} p_G \\ p_L \end{bmatrix} + \frac{1}{U_N} \Im \begin{bmatrix} M & N \\ N^T & Q \end{bmatrix} \begin{bmatrix} q_G \\ q_L \end{bmatrix} + \mathbf{1}U_N. \quad (8)$$

Equation (8) represents a more general version of the widely used *linearized DistFlow model* (e.g. in [8], [9], [11]), which holds also in the case of no radial grids. Equations (7) and (8) will be used in the following to model the grid voltages and their magnitude, respectively.

IV. VOLTAGE CONTROL STRATEGIES BASED ON REACTIVE POWER REGULATION

Classically, the generators regulate the amount of reactive power they inject into the electrical grid, in order to perform the *voltage control*, i.e., to maintain the voltage magnitudes of the buses within a predefined deviation from the nominal voltage U_N . Since we assume that only agents can take voltage measurements, we aim at meeting the following constraints

$$U_{\min} \leq v_h \leq U_{\max}, \quad \forall h \in \mathcal{C}. \quad (9)$$

where U_{\min} and U_{\max} denote, respectively, the minimum and maximum admissible values for the voltages magnitude. Usually, $U_{\min} = (1 - \xi)U_N$ and $U_{\max} = (1 + \xi)U_N$, where $0 < \xi < 1$.

In addition, since typically the generators dispersed in the distribution network are of small size, we take into account also constraints on the generation capability of agent h . Specifically, we assume

$$q_{\min,h} \leq q_h \leq q_{\max,h}, \quad \forall h \in \mathcal{C}, \quad (10)$$

where $q_{\min,h}$, $q_{\max,h}$ are, respectively, the minimum and the maximum amount of reactive power that agent h can inject. Typically $q_{\min,h} < 0$, $q_{\max,h} > 0$ and $q_{\min,h} = -q_{\max,h}$. For the sake of simplicity and in order to keep the notation lighter, in the following, we will assume that the micro-generators are homogeneous, namely, for all $h \in \mathcal{C}$,

$$q_{\min,h} = q_{\min}, \quad q_{\max,h} = q_{\max}, \quad (11)$$

for given q_{\min} , q_{\max} . Based on the constraints in (9) and in (10), we introduce a proper definition of the set of the *feasible reactive power injections*. Observe that, in the setup we described, the quantities p_G , p_L and q_L are assumed to be constant and that only q_G is actuated in order to regulate v_G . Hence, for a given triple (p_G, p_L, q_L) , we define

$$\mathcal{F}(p_G, p_L, q_L) = \{q_G \text{ such that for all } h \in \mathcal{C} \text{ it holds } q_{\min} \leq q_h \leq q_{\max}, U_{\min} \leq v_h \leq U_{\max}\}.$$

Since there is no risk of confusion, for the sake of notational convenience, we omit the dependence of \mathcal{F} on (p_G, p_L, q_L) .

In next sections we introduce three strategies, where each agent updates the amount of reactive power to be injected in

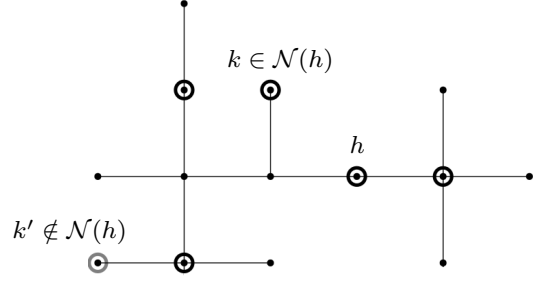


Figure 2. An example of neighboring cyber layer agents. Circled nodes (both black and gray) represent agents (nodes belonging to \mathcal{C}). The black circled nodes belong to the set of neighbors of h . The gray circled node is an agent that do not belong to the set $\mathcal{N}(h) \subset \mathcal{C}$. For each agent $k \in \mathcal{N}(h)$, there exists a path that connects h to k which does not include any other agent.

order to maintain the voltages magnitudes within the interval $[U_{\min}, U_{\max}]$. The first two strategies are *purely local*, i.e.,

- 1) agent h updates q_h based only on measurements of the magnitude of its own voltage, that is, v_h ;
- 2) there is no exchange of information between the agents.

In the third strategy, instead, agents can communicate with each other; the exchange of information regards the taken measurements and some additional quantities, as we will describe in Section VI. To properly model the admissible communications in the cyber layer, we next define the set of neighbors of a given agent h .

Definition 1: Let $h \in \mathcal{C}$ be an agent. The set of neighbors of h , denoted as $\mathcal{N}(h)$, is the subset of \mathcal{C} defined as

$$\mathcal{N}(h) = \{k \in \mathcal{C} \cup \{1\} \mid \exists \mathcal{P}_{hk}, \mathcal{P}_{hk} \cap \mathcal{C} = \{h, k\}\}.$$

In Figure 2 we report an example of the neighbors set. In our setup we assume that every agent $h \in \mathcal{C}$ knows its neighbors, i.e., $\mathcal{N}(h)$, and that it can communicate with them.

V. PURELY LOCAL VOLTAGE CONTROL STRATEGIES

In this section we propose two control strategies where each agent h updates q_h exploiting only measurements of its own voltage magnitude, i.e., v_h .

A. A first local voltage control strategy (denoted as LVC-1)

LVC-1 is a modified version of the reactive power compensation technique introduced in [4]. To formally describe LVC-1, let $f(v)$ be defined as

$$f(v) = \zeta v + \beta \quad (12)$$

where

$$\zeta = -\frac{q_{\max} - q_{\min}}{U_{\max} - U_{\min}}, \quad \beta = \frac{q_{\max}U_{\max} - q_{\min}U_{\min}}{U_{\max} - U_{\min}}$$

In addition, let $\hat{f}(v)$ be the saturated version of $f(v)$ outside the interval $[q_{\min}, q_{\max}]$, that is,

$$\hat{f}(v) = [f(v)]_{q_{\min}}^{q_{\max}}. \quad (13)$$

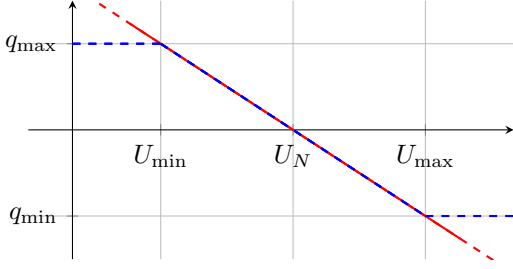


Figure 3. Pictorial representation of f (red solid line) and \hat{f} (blue dashed line), in the particular case where $q_{\max} = q_{\min}$ and $U_{\min} = (1 - \xi)U_N$, $U_{\max} = (1 + \xi)U_N$.

In Figure 3, we provide a pictorial representation of f and \hat{f} . After having taken the measurement $v_h(t)$, $q_h(t)$ is updated by the h -th agent in the following way

$$q_h(t+1) = [q_h(t) + \alpha (f(v_h(t)) - q_h(t))]_{q_{\min}}^{q_{\max}} \quad (14)$$

where α is a positive constant. Observe that the equilibrium points for Equation (14) are described by $\hat{f}(v)$; in fact, if $q_h(t) = \hat{f}(v_h(t))$ then $q_h(t+1) = q_h(t)$. Moreover, if $q_{\min} = -q_{\max}$, $U_{\min} = (1 - \xi)U_N$ and $U_{\max} = (1 + \xi)U_N$, then

$$\zeta = -\frac{q_{\max}}{\xi U_N}, \quad \beta = \frac{q_{\max}}{\xi},$$

and it holds true that $\hat{f}(U_N) = 0$. The following Proposition characterizes the convergence properties of (14).

Proposition 1: Consider algorithm (14). Then, if

$$\alpha \leq \frac{2}{1 - \frac{\zeta \rho(\mathfrak{S}(M))}{U_N}}, \quad (15)$$

there exists a m -upla $(\bar{v}_1, \dots, \bar{v}_m)$ such that $v_h(t) \rightarrow \bar{v}_h$ and $q_h(t) \rightarrow \hat{f}(\bar{v}_h)$ for all $h \in \{1, \dots, m\}$.

Although LVC-1 is based on the quite popular voltage control strategy introduced in [4], in general, it does not guarantee that \bar{v}_h lies within the interval $[U_{\min}, U_{\max}]$. If α satisfies condition (15), then each v_h converges to a steady-state \bar{v}_h that, in general, might violate the constraints (9). In Section VII, we will provide a numerical example where, for some h , $\bar{v}_h \notin [U_{\min}, U_{\max}]$.

Remark 1: As previously said, LVC-1 is based on the strategy proposed in [4], which complies also the IEEE 1547.8 standard [16]. In [4] q_h is updated as follows

$$q_h(t+1) = \hat{f}(v_h(t)), \quad (16)$$

i.e., q_h is set directly equal to the value dictated by the function \hat{f} . However, as remarked also by the authors of [4], the practical execution of (16) could lead to oscillatory and unstable behaviors which are avoided by the *integral* rule (14).

Remark 2: Other purely local strategies have been proposed in the literature. The algorithm in [8] is probably shown to drive the voltages into the operating intervals defined in (9); however the analysis in [8] is carried on only in the limited scenario where all the agents are assumed to be compensators and where no limits on the reactive powers are taken into account. Instead, the algorithms proposed in [10], [11] assume

the constraints in (10) to hold for all the compensators; these algorithms, similarly to LVC-1 are theoretically proved to converge to a steady-state which, however, is not guaranteed to satisfy the voltages' constraints.

B. A second local voltage control strategy (denoted as LVC-2)

LVC-2 aims at driving all the compensators' voltage magnitudes to a desired value U_d . Again it is based only on local measurements, but differently from LVC-1, it does not resort to a droop-like function as the one introduced in (13). Specifically, agent h updates the amount of reactive power to be injected as

$$q_h(t+1) = [q_h(t) + \epsilon (U_d - v_h(t))]_{q_{\min}}^{q_{\max}} \quad (17)$$

where ϵ is a positive constant. Loosely speaking, the rationale behind LVC-2 is as follows: if $v_h < U_d$ then agent h will inject reactive power in order to increase v_h , while if $v_h > U_d$ then agent h will absorb reactive power in order to decrease v_h . The convergence properties of LVC-2 are next stated.

Proposition 2: Consider algorithm (17). Then, if

$$\epsilon \leq \frac{2U_N}{\rho(\mathfrak{S}(M))} \quad (18)$$

there exist a m -upla $(\bar{v}_1, \dots, \bar{v}_m)$ such that $v_h(t) \rightarrow \bar{v}_h$ for all $h \in \{1, \dots, m\}$.

The proof of Proposition 2 is reported in Appendix A. Observe that the above Proposition establishes that, if ϵ satisfies condition (18), then the voltages magnitudes converge to steady state values $(\bar{v}_1, \dots, \bar{v}_m)$. However, in general, it is not guaranteed that $\bar{v}_h = U_d$ for all $h \in \{1, \dots, m\}$, and that $\bar{v}_h \in [U_{\min}, U_{\max}]$ even if $U_d \in [U_{\min}, U_{\max}]$. In Section VII we will provide a numerical example where, though $U_d \in [U_{\min}, U_{\max}]$, there exists at least one agent h such that $\bar{v}_h \notin [U_{\min}, U_{\max}]$.

VI. A FAST DISTRIBUTED OPTIMAL REACTIVE POWER FLOW ALGORITHM (DENOTED AS F-DORPF)

In this section, we propose a novel *distributed* control algorithm where each agent h , beside local voltage measurements, requires additional information coming from the neighboring nodes in $\mathcal{N}(h)$ to update the amount of reactive power it injects. In addition to a voltage regulation objective, the strategy exploits the cooperation among the agents to minimize the power losses on the electric lines; specifically, it aims at solving the following *optimal reactive power flow* (OPRF) problem

$$\min_{q_G} \Re(\bar{u}^T Y u) \quad (19a)$$

$$\text{subject to } q_G \in \mathcal{F} \quad (19b)$$

where $\Re(\bar{u}^T Y u)$ are the line active power losses. Indeed, in [15] it is shown how, by exploiting (7), the line power losses can be expressed by (19a). The algorithm is derived in the simplified scenario where all the grid power lines are assumed to have the same resistance/inductance ratio, i.e., there exists θ , such that

$$z_e = e^{i\theta} |z_e|. \quad (20)$$

for all $e \in \mathcal{E}$. Equation (20) is satisfied when the grid is relatively homogeneous, and is reasonable in most practical cases. However, in Section VII, we simulate the algorithm in the more realistic scenario where (20) does not hold. It can be shown (see [15] for the details) that, under approximation (7) and under (20), the cost function (19a) is a quadratic function on q_G and \mathcal{F} is a convex set on q_G . Indeed, we have that

$$\Re(\bar{u}^T Y u) \simeq q_G^T \frac{\Re(M)}{U_N^2} q_G + 2q_G^T \frac{\Re(N)}{U_N^2} q_L + q_L^T \frac{\Re(Q)}{U_N^2} q_L,$$

and that \mathcal{F} can be conveniently approximated by

$$\tilde{\mathcal{F}} = \left\{ q_G : V_{\min} \leq \frac{\Im(M)}{U_N} q_G \leq V_{\max}, q_{\min} \leq q_G \leq q_{\max} \right\}$$

where

$$V_{\min} = -\frac{1}{U_N} \left(\Re[M \quad N] \begin{bmatrix} p_G \\ p_L \end{bmatrix} - \Im(N) q_L \right) + \mathbf{1}(U_{\min} - U_N),$$

$$V_{\max} = -\frac{1}{U_N} \left(\Re[M \quad N] \begin{bmatrix} p_G \\ p_L \end{bmatrix} - \Im(N) q_L \right) + \mathbf{1}(U_{\max} - U_N).$$

Therefore, problem (19) can be convexified obtaining

$$\min_{q_G} q_G^T \frac{\Re(M)}{U_N^2} q_G + 2q_G^T \frac{\Re(N)}{U_N^2} q_L + q_L^T \frac{\Re(Q)}{U_N^2} q_L \quad (21a)$$

$$\text{subject to } q_G \in \tilde{\mathcal{F}} \quad (21b)$$

We refer to the above problem as the *approximated convexified (OPRF) problem* and we denote by q_G^* its optimal solution.

The f-DORPF algorithm improves the performance of the algorithm presented in [15] (denoted hereafter as DORPF). DORPF addresses problem (19) by a iterative dual ascent strategy adopting auxiliary variables, i.e., the *Lagrange multipliers*, for both the voltage and the reactive power constraints.

Differently from LVC-1 and LVC-2, agents in DORPF can communicate with their neighbors. Remarkably, it is shown in [15] that, under (7), (20) and some additional mild assumptions, DORPF converges to q_G^* , i.e., the optimal solution of the approximated convexified OPRF problem. In other words, thanks to the additional information received from the neighbors, the agents not only drive the voltage magnitudes to satisfy the operational constraints, but also minimize the power losses. However, in spite of this optimal steady-state property, experimental results show how the transient of DORPF is much slower than the one of the local algorithms.

In this Section, to improve the transient performance, we introduce the f-DORPF algorithm, obtained by combining DORPF with LVC-2. Numerical results reported in Section VII show how f-DORPF inherits the fast transient of LVC-2 and the convergence to the optimal equilibrium of DORPF. The f-DORPF algorithm is still an iterative dual-ascent like strategy where only the Lagrange multipliers associated to the reactive power constraints are introduced. Eliminating the Lagrange multipliers related to voltages' constraints speeds up significantly the transient of the DORPF algorithm; in f-DORPF, the absence of the voltages' multipliers is compensated by the fact that agent h performs a step of LVC-2 whenever $v_h < U_{\min}$ or $v_h > U_{\max}$.

An algorithmic description of f-DORPF is provided in Algorithm 1 where, for each agent h , $\mu_{\min,h}$ and $\mu_{\max,h}$ denote the

Lagrange multipliers associated with the constraints $q_h \geq q_{\min}$ and $q_h \leq q_{\max}$, respectively. Moreover, the symbol $y_{h,\ell}$ denotes the admittance of the electrical path between agents h and ℓ which is assumed to be known by both agent h and agent ℓ . Also the positive parameters ϵ and γ are assumed to be a-priori assigned (in particular, ϵ satisfying (18)).

Algorithm 1 f-DORPF

Require: At each time t , agent h

- 1: gathers $\mu_k(t-1)$, $k \in \mathcal{N}(h)$, and measures $u_h(t)$, $v_h(t)$.
- 2: **if** $v_h(t) \geq U_{\max}$ or $v_h(t) \leq U_{\min}$ **then**
- 3:
$$\delta_h = \epsilon(U_N - v_h(t)) \quad (22)$$

4: **end if**

5: **if** $U_{\min} < v_h(t) < U_{\max}$ **then**

6: computes

$$\delta_{f,h} = \sum_{\ell \in \mathcal{N}(h)} \left(\mu_{\min,\ell}(t) - \mu_{\max,\ell}(t) + y_{h,\ell} v_h(t) v_\ell(t) \sin(\angle u_\ell(t) - \angle u_h(t) - \theta) \right) \quad (23)$$

$$\delta_{U_{\max},h} = \epsilon(U_{\max} - v_h(t)) \quad (24)$$

$$\delta_{U_{\min},h} = \epsilon(U_{\min} - v_h(t)) \quad (25)$$

and sets

7: **if** $\text{sign}(\delta_{U_{\min},h}) = \text{sign}(\delta_{f,h})$ **then**

8: $\tilde{\delta} = \delta_{U_{\min},h}$

9: **else**

10: $\tilde{\delta} = \delta_{U_{\max},h}$

11: **end if**

12:

$$\delta_h = \text{sign}(\delta_{f,h}) \min\{\delta_{f,h}, \tilde{\delta}\} \quad (26)$$

13: **end if**

14: computes the reactive power update

$$\tilde{q}_h = q_h(t) + \delta_h \quad (27)$$

15: computes the Lagrange multipliers update

$$\mu_{\min,h}(t+1) = \left[\mu_{\min,h}(t) + \gamma \left(\frac{q_{\min}}{U_N^2} - \frac{\tilde{q}_h}{U_N^2} \right) \right]_0^\infty \quad (28)$$

$$\mu_{\max,h}(t+1) = \left[\mu_{\max,h}(t) + \gamma \left(\frac{\tilde{q}_h}{U_N^2} - \frac{q_{\max}}{U_N^2} \right) \right]_0^\infty \quad (29)$$

16: injects the projected setpoints

$$q_h(t+1) = [\tilde{q}_h]_{q_{\min}}^{q_{\max}} \quad (30)$$

Some explanations are in order. If v_h violates constraint (9), agent h updates its reactive power by using the LVC-2 rule, once set $U_d = U_N$ (see equation (22)).

Instead, if $v_h \in [U_{\min}, U_{\max}]$, then agent h discriminates between a step inspired by DORPF (see equation (23) and the algorithm presented in Section VI in [15]), and a step of LVC-2 (see equations (24) and (25) obtained by setting, respectively, $U_d = U_{\max}$ and $U_d = U_{\min}$). Observe that the term $\delta_{f,h}$ involves the knowledge of multipliers of h and of its neighbors; therefore its computation requires the communication between

neighboring agents. Of note, the update rule of q_h based only on $\delta_{f,h}$ has been proposed and fully analyzed in [17], where, however, the goal was only the power loss minimization, without considering any voltage support to the grid. Notice that the terms $\delta_{U_{\max},h}$ and $\delta_{U_{\min},h}$ have, by definition, different signs. Let $\tilde{\delta}$ be the one with the same sign of $\delta_{f,h}$. The h 's reactive power increments $\delta_{f,h}$ and $\tilde{\delta}$ would have the same effect on h 's voltage magnitude: either an increment (if both positive) or a decrement (if both negative). To keep the constraints satisfied, f-DORPF chooses the less aggressive update between $\delta_{f,h}$ and $\tilde{\delta}$ (see equation (26)): indeed, as discussed in [17], the mere use of (23) could drive the voltage magnitudes outside the range $[U_{\min}, U_{\max}]$, though moving the system towards the minimum losses configuration. This is the reason why we can not simply rely on (23), but, instead, we propose an update based on the choice in (26).

We conclude this subsection by highlighting another interesting property of the f-DORPF. Agent h updates the Lagrange multipliers $\mu_{\min,h}$, $\mu_{\max,h}$ (by (28) and (29)) at each iteration of the algorithm, also when the value of δ_h does not depend on $\mu_{\min,h}$ or $\mu_{\max,h}$, i.e., when the amount of reactive power to be injected is computed according to a LVC-2 step. Nonetheless, the updated values of $\mu_{\min,h}$ and $\mu_{\max,h}$ are broadcasted to agents in $\mathcal{N}(h)$, that use them to perform computations in (23); likely, some of the reactive power set points computed by agents in $\mathcal{N}(h)$ will depend on these values of $\mu_{\min,h}$ and $\mu_{\max,h}$. This information flow is crucial to meet the operative constraints; indeed it is thanks to this cooperation that agents are able to rise or decrease the voltage magnitude of those agents, which are operating at their limits (in terms of reactive power injection), but are violating the voltage constraints.

A. On the equilibrium points of the f-DORPF

In the following Proposition we characterize the equilibrium points of the f-DORPF algorithm by assuming that the grid is radial, which is always the case of distribution networks.

Proposition 3: Consider the f-DORPF algorithm and assume the grid radial. Let q_G^* be the optimal solution of the approximated convexified OPF problem. Then the following two facts hold true:

- 1) There exist $(\mu_{\max}^*, \mu_{\min}^*)$ such that $(q_G^*, \mu_{\max}^*, \mu_{\min}^*)$ is an equilibrium for the f-DORPF; and
- 2) If $(\tilde{q}_G, \tilde{\mu}_{\max}, \tilde{\mu}_{\min})$ is an equilibrium for the f-DORPF, then $\tilde{q}_G = q_G^*$.

The proof of the proposition is reported in Appendix A. Observe that the above Proposition ensures the existence of equilibrium points for the f-DORPF and that the component of the reactive power of these equilibria coincides with q_G^* .

VII. SIMULATIONS AND DISCUSSION

The algorithms have been simulated on testbeds inspired from the IEEE 37 and the IEEE 123 (see [18]), depicted in Figure 4 and 5. Notice that both the assumptions on homogeneous micro-generators and homogeneous line impedances do not hold, i.e. both (11) and (20) are not satisfied. Thus, the algorithms are tested in a realistic scenario. We consider the scenario where several micro-generators, gray nodes in

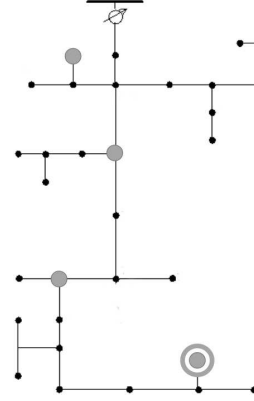


Figure 4. Schematic representation of the IEEE 37 test feeder [18], the agents are represented by gray nodes in the distribution network.

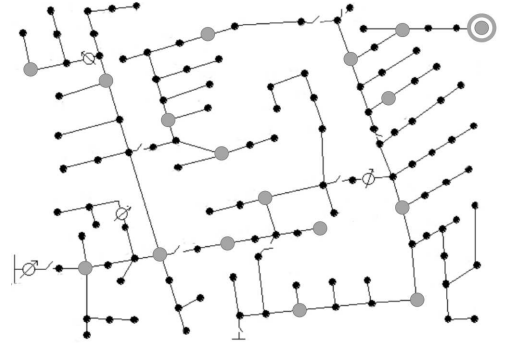


Figure 5. Schematic representation of the IEEE 123 test feeder [18], the agents are represented by gray nodes in the distribution network.

Figure 4 and 5, can regulate the reactive power injection to control the voltage magnitude. The algorithms presented have been run on a nonlinear exact solver of the grid [19]. In all the simulations, the reactive power outputs of the micro-generators have been initialized to zero, while their generation capabilities have been chosen in such a configuration guaranteeing that the constraints (9) are satisfied, always exists, i.e., the system is always feasible. The simulations have been obtained optimizing over the parameters α , ϵ and γ .

A. Static load analysis

In this subsection we compare the algorithms performance when the grid loads are time-invariant. In Figure 6 and 7 we plot, for each strategy, the voltage magnitude profile of the agent achieving the smallest value at the steady state, i.e., the agents which are circled in Figure 4 and 5¹. Notice that, though the system is feasible, LVC-1 and LVC-2 fail to meet the voltage magnitude constraints in the IEEE37 case (see Figure 6). Nonetheless, the general effect of LVC-1 and LVC-2 is that of moving the voltage magnitude towards the feasible set; indeed, the distance of the steady-state voltage magnitude from U_{\min} is smaller than the distance of the initial

¹For simplicity we consider only the constraint $v_h \geq U_{\min}$.

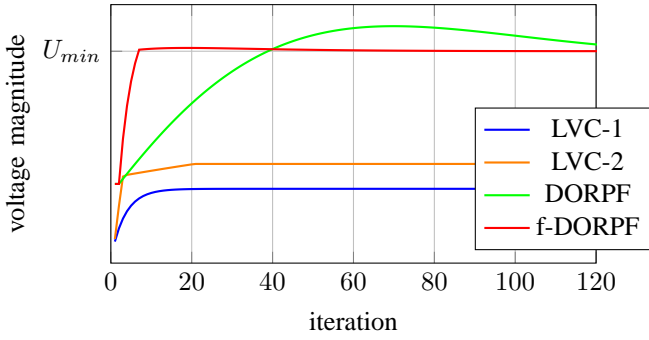


Figure 6. Minimum compensators voltage magnitude using the algorithms presented in the IEEE37 test case.

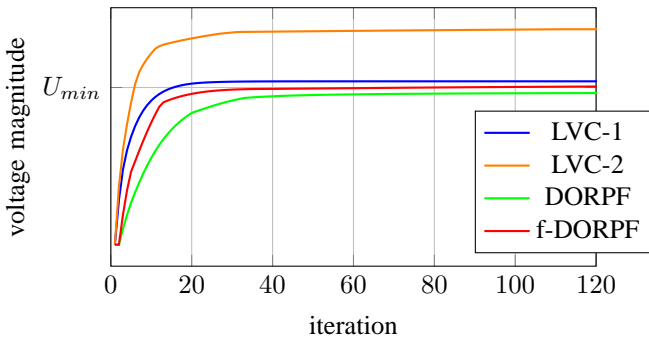


Figure 7. Minimum compensators voltage magnitude using the algorithms presented in the IEEE123 test case.

voltage magnitude from U_{\min} . In Figure 7 all the strategies lead the voltage magnitude within $[U_{\min}, U_{\max}]$; in this case, we highlight the fast transient of LVC-1, LVC-2 and how f-DORPF significantly improves the performance of DORPF.

In Figure 8 we report the behavior of the power losses in the IEEE37 test case. Observe that f-DORPF attains the same steady-state value of the DORPF, exhibiting a faster transient. Instead, LVC-1 and LVC-2, since they do not aim at minimizing the losses, lead the system to a less efficient configuration.

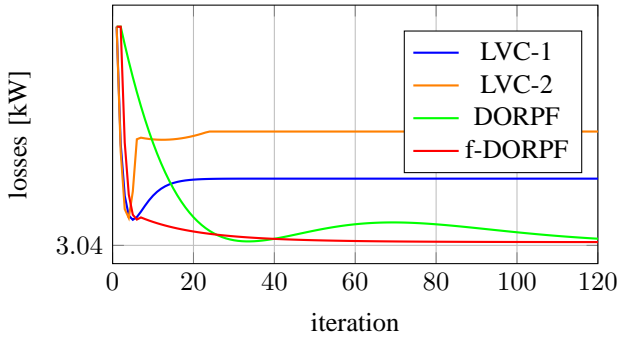


Figure 8. System losses using the DORPF and the f-DORPF. The losses minimum value of this particular realization, computed via a centralized solver, is of 3.04 kW

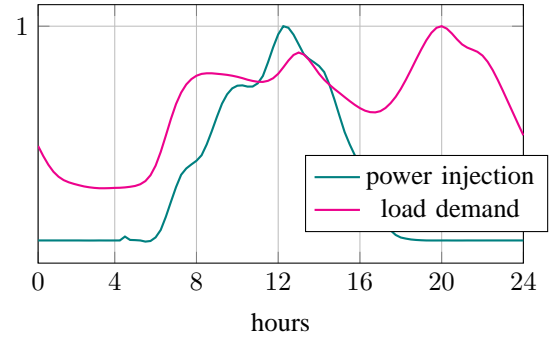


Figure 9. Daily behaviour of power generation and of load demand

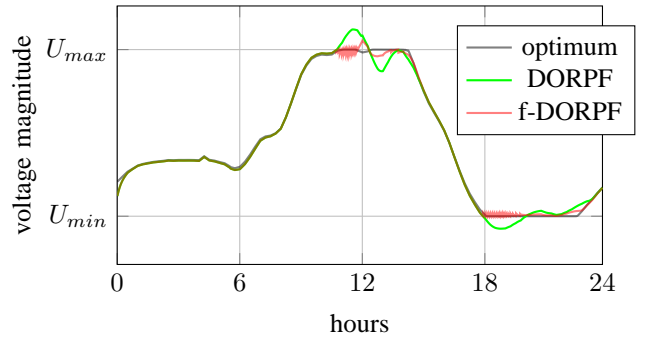


Figure 10. Voltage magnitude profile of the circled agent in Figure 4

B. Dynamic load analysis

In this subsection we compare algorithms performance when the loads are time varying. In Figure 9 we plot the daily profiles, that we consider in our simulations, of both the total load demand (purple line) and of the total active power injected by the agents into the grid (blue line). Both profiles are normalized with the respect to the maximum value assumed during the day.

Typically, the inverter of agent h has an instantaneous generation capability which is limited by its fixed apparent power capability $|s_{\max,h}|$; namely, the phasor representing the instantaneous power injected must lie inside a circle of ray $|s_{\max,h}|$ centered at the origin. In our simulations, we assume

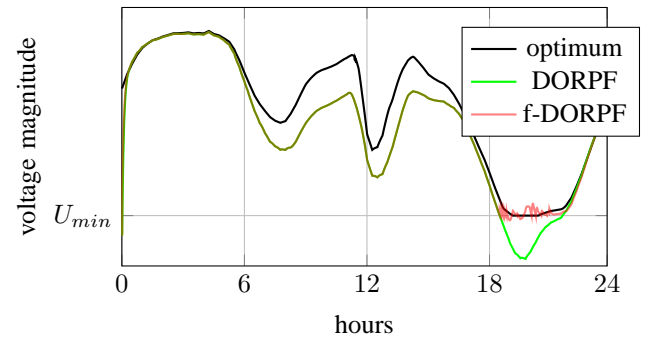


Figure 11. Voltage magnitude profile of the circled agent in Figure 5

$|s_{\max,h}| = 1.1p_{\max,h}$, where $p_{\max,h}$ is the maximum amount of active power that can be generated, as suggested in [7], since inverters are available in discrete sizes and are likely to be slightly oversized with the respect to $p_{\max,h}$. It turns out that the amount of reactive power that can be injected by agent h at time t is a function of $|s_{\max,h}|$ and of the injected active power $p_h(t)$, i.e.,

$$q_{\max,h}(t) = \sqrt{|s_{\max,h}|^2 - p_h(t)^2}$$

and $q_{\min,h}(t) = -q_{\max,h}(t)$. In our setup we have verified that \mathcal{F} is nonempty for any t , namely there is always a feasible solution. In our simulations, the control actions are performed every 30 seconds. The results are reported in Figure 10 and 11, where we plotted the daily behavior of the voltage magnitude of the circled agent in the IEEE37 and in the IEEE123 testbeds, respectively. The optimal solution computed through a centralized solver.

The following observations are in order. Firstly, when there are no voltage constraints violations, the trajectories described by DORPF and f-DORPF are basically the same; in other words f-DORPF acts as DORPF, thus attaining power losses minimization. Secondly, during the central hours of the day, in the IEEE37 testbed an overvoltage occurs due to the massive increment of active power injected. Notice that, it takes a while for DORPF to drive the voltage magnitude below the limit value U_{\max} ; instead, f-DORPF is able to keep the constraints satisfied (i.e., the overvoltage is avoided) and generates a trajectory which is very close to the optimal one. Thirdly, during evening hours, the injection of active power significantly decreases causing an undervoltage. Again f-DORPF exhibits a superior performance with the respect to DORPF; no undervoltage appears in the trajectory depicted by f-DORPF, while it is not avoided when DORPF is adopted.

The better performance of f-DORPF in tracking the optimal solution in the more realistic scenario of time-varying loads, is related to its faster transient property we highlighted in the previous numerical example and in Section VI.

VIII. CONCLUSIONS

In this paper we propose and analyze, theoretically and through simulations, three voltage control strategies. The LVC-1 and the LVC-2 algorithms are purely local: the agents regulate their reactive power output based only on the knowledge of the magnitude of their own voltage. Since they do not require any communication infrastructure, they can be easily implemented but it is not guaranteed that the voltage constraints are met. Instead, the f-DORPF algorithm is distributed: the reactive power setpoints are computed by the agents exploiting both local measurements and information coming from the neighbors. This cooperation is exploited to not only satisfy the voltage requirements, but also to achieve the power losses optimality. The f-DORPF has been designed by combining DORPF (a distributed algorithm presented in [15] solving the optimization problem (21)) and LVC-2. Specifically, f-DORPF inherits the fast transient of LVC-2 and the steady state optimality property of DORPF. Simulations, illustrating the effectiveness of f-DORPF, are provided.

APPENDIX

The component wise reactive power update (14) can be expressed in vectorial form as

$$q_G(t+1) = \left[\left(I + \frac{\alpha \zeta \mathfrak{S}(M)}{U_N} - \alpha I \right) q_G(t) + \alpha \zeta \tilde{V} + \alpha \beta \right]_{q_{\min}}^{q_{\max}} \quad (31)$$

where

$$\tilde{V} = \frac{\mathfrak{S}(N)}{U_N} q_L + \frac{\Re[M \quad N]}{U_N} \begin{bmatrix} p_G \\ p_L \end{bmatrix} + \mathbf{1} U_N. \quad (32)$$

Notice that \tilde{V} represents the contribution of the uncontrolled powers p_G, p_L, q_L to the agents voltage magnitude, i.e.

$$v_G = \frac{\mathfrak{S}(M)}{U_N} q_G + \tilde{V}.$$

Let us define $x(t) = q_G(t) - q_G(k-1)$. By exploiting the fact that given the vectors v, w, a, b and $\| [v]_a^b - [w]_a^b \| \leq \| v - w \|$, it can be easily shown that

$$\| x(t+1) \| \leq \left\| \left(I + \frac{\alpha \zeta \mathfrak{S}(M)}{U_N} - \alpha I \right) \right\| \| x(t) \| \quad (33)$$

From equation (33), it trivially follows that if

$$\alpha \leq \frac{2}{1 - \frac{\zeta \rho(\mathfrak{S}(M))}{U_N}},$$

then $\| x(t) \| \rightarrow 0$ and then $q_G(t) \rightarrow \bar{q}_G$, i.e. the reactive power injected reaches the equilibrium \bar{q}_G , associated with the voltages $(\bar{u}_1, \dots, \bar{u}_m)$.

The component wise reactive power update (17) can be expressed in vectorial form as

$$q_G(t+1) = \left[\left(I - \frac{\epsilon \mathfrak{S}(M)}{U_N} \right) q_G(t) + \epsilon (u_d - \tilde{V}) \right]_{q_{\min}}^{q_{\max}}, \quad (34)$$

where \tilde{V} is the same defined in equation (32). Similarly to what done before, let us define $x(t) = q_G(t) - q_G(k-1)$. Then

$$\begin{aligned} \| x(t+1) \| &\leq \left\| \left(I - \frac{\epsilon \mathfrak{S}(M)}{U_N} \right) x(t) \right\| \\ &\leq \left\| I - \frac{\epsilon \mathfrak{S}(M)}{U_N} \right\| \| x(t) \| \end{aligned} \quad (35)$$

It is thus straightforward to see that if condition (18) holds, $\| x(t) \| \rightarrow 0$ then $q_G(t) \rightarrow \bar{q}_G$, i.e. the reactive power injected reaches the equilibrium \bar{q}_G , associated with the voltages $(\bar{u}_1, \dots, \bar{u}_m)$.

Consider problem (21). Observe that it can be solved through the standard *dual ascent* strategy, whose iterative updating equations are the following:

$$\begin{aligned} q_G(t+1) &= q_G(t) + \delta_D (q_G(t), \lambda_{\min}(t), \lambda_{\max}(t), \\ &\quad \mu_{\max}(t), \mu_{\min}(t)) \\ \lambda_{\min,h}(t+1) &= \left[\lambda_{\min,h}(t) + \frac{\gamma}{U_N^2} (U_{\min}^2 - v_h(t)^2) \right]_0^\infty \\ \lambda_{\max,h}(t+1) &= \left[\lambda_{\max,h}(t) + \frac{\gamma}{U_N^2} (v_h(t)^2 - U_{\max}^2) \right]_0^\infty \\ \mu_{\min,h}(t+1) &= \left[\mu_{\min,h}(t) + \frac{\gamma}{2U_N^2} (q_{\min} - \bar{q}_h) \right]_0^\infty \\ \mu_{\max,h}(t+1) &= \left[\mu_{\max,h}(t) + \frac{\gamma}{2U_N^2} (\bar{q}_h - q_{\max}) \right]_0^\infty \end{aligned}$$

The expression of $\delta_D(q_G, \lambda_{\min}, \lambda_{\max}, \mu_{\max}, \mu_{\min})$ has been derived in [15], and is given by

$$\begin{aligned} \delta_D(q_G, \lambda_{\min}, \lambda_{\max}, \mu_{\max}, \mu_{\min}) = & \\ & -q_G - M^{-1}Nq_L + \sin\theta(\lambda_{\min} - \lambda_{\max}) \\ & + M^{-1}(\mu_{\min} - \mu_{\max}). \end{aligned} \quad (36)$$

Since problem (21) is convex, standard optimization results (see [20]) show that, for suitable values of γ , the dual ascent strategy converges to $(q_G^*, \lambda_{\min}^*, \lambda_{\max}^*, \mu_{\min}^*, \mu_{\max}^*)$, being q_G^* the optimizer of problem (21). Let δ_f be the vector collecting all the $(\delta_f)_h$'s (defined in equation (23)), $h \in \mathcal{C}$. The vector δ_f can be expressed (see [15]) as

$$\begin{aligned} \delta_f = \Im \left(e^{-j\theta} \text{diag}(\bar{u}_G) [M^{-1}\mathbf{1} \quad M^{-1}] \begin{bmatrix} u_0 \\ u_G \end{bmatrix} \right) \\ + M^{-1}(\mu_{\min} - \mu_{\max}). \end{aligned} \quad (37)$$

Exploiting the linear model (8), it can be shown that equation (37) can be rewritten as

$$\begin{aligned} \delta_f(q_G, \lambda_{\min}, \lambda_{\max}, \mu_{\max}, \mu_{\min}) = & -q_G - M^{-1}Nq_L \\ & + M^{-1}(\mu_{\min} - \mu_{\max}). \end{aligned} \quad (38)$$

Let the equilibrium of the dual ascent strategy be $(q_G^*, \lambda_{\min}^*, \lambda_{\max}^*, \mu_{\min}^*, \mu_{\max}^*)$. It satisfies the condition

$$\delta_D(q_G^*, \lambda_{\min}^*, \lambda_{\max}^*, \mu_{\min}^*, \mu_{\max}^*) = 0.$$

We will show that $(q_G^*, \mu_{\min}^*, \mu_{\max}^*)$ is an equilibrium for the f-DORPF. Let h denote an agent whose multipliers $\lambda_{\min,h}^*, \lambda_{\max,h}^*$ are equal to zero. In this case, by comparing (36) and (38), it follows that

$$\begin{aligned} \delta_f(q_G^*, \mu_{\min}^*, \mu_{\max}^*) \\ = \delta_D(q_G^*, \lambda_{\min}^*, \lambda_{\max}^*, \mu_{\min}^*, \mu_{\max}^*) \\ = 0. \end{aligned}$$

As a consequence, we have, from (26), that $\delta_h = 0$ for all $h \in \mathcal{C}$.

Now, let h denote an agent such that either $\lambda_{\min,h}^*$ or $\lambda_{\max,h}^*$ is greater than zero. This implies that v_h is equal to either U_{\min} or U_{\max} . Consider the case where $\lambda_{\min,h}^* > 0$ and $v_h = U_{\min}$ (the case where $\lambda_{\max,h}^* > 0$ and $v_h = U_{\max}$ is analogous). Being $v_h = U_{\min}$, from (24) and (25) it turns out that $\delta_{U_{\max},h} > 0$ and $\delta_{U_{\min},h} = 0$. Furthermore,

$$\begin{aligned} \delta_{f,h}(q^*, \mu_{\min}^*, \mu_{\max}^*) \\ \leq \delta_{D,h}(q^*, \mu_{\min}^*, \mu_{\max}^*, \lambda_{\min}^*, \lambda_{\max}^*) = 0. \end{aligned}$$

From (26), it follows that $\delta_h = 0$. Thus $(q_G^*, \mu_{\min}^*, \mu_{\max}^*)$ is an equilibrium for the f-DORPF.

On the converse, let $(\tilde{q}_G, \tilde{\mu}_{\min}, \tilde{\mu}_{\max})$ be an equilibrium of the f-DORPF algorithm. Firstly, notice that \tilde{q}_G belongs to $\tilde{\mathcal{F}}$. In fact, if $\tilde{q}_G \notin \tilde{\mathcal{F}}$, then there would be at least an agent h such that either $v_h < U_{\min}$ and $q_h = q_{\max}$, or $v_h > U_{\max}$ and $q_h = q_{\min}$. Consider the former case (the latter is analogous). From (??) and (29), it follows that $\tilde{\mu}_{\max,h}$ keeps increasing, and thus $(\tilde{q}_G, \tilde{\mu}_{\min}, \tilde{\mu}_{\max})$ is not an equilibrium. Hence $\tilde{q}_G \in \tilde{\mathcal{F}}$. Now,

let us introduce the auxiliary variables $\tilde{\lambda}_{\min}$ and $\tilde{\lambda}_{\max}$, defined as

$$\begin{aligned} \tilde{\lambda}_{\min,h} &= \begin{cases} 0 & \text{if } \delta_{f,h} \geq 0 \\ -\frac{\delta_{f,h}}{\sin\theta} & \text{if } \delta_{f,h} < 0 \end{cases} \\ \tilde{\lambda}_{\max,h} &= \begin{cases} 0 & \text{if } \delta_{f,h} \leq 0 \\ \frac{\delta_{f,h}}{\sin\theta} & \text{if } \delta_{f,h} > 0 \end{cases} \end{aligned}$$

Observe that both $\tilde{\lambda}_{\min}$ and $\tilde{\lambda}_{\max}$ have only non-negative entries and that

$$\delta_D(\tilde{q}_G, \tilde{\lambda}_{\min}, \tilde{\lambda}_{\max}, \tilde{\mu}_{\min}, \tilde{\mu}_{\max}) = 0.$$

Thus, since the minimizer is unique, $\tilde{q}_G = q_G^*$.

REFERENCES

- [1] A. Ipakchi and F. Albuyeh, "Grid of the future," *IEEE Power and Energy Magazine*, vol. 7, no. 2, pp. 52–62, 2009.
- [2] F. Katiraei and M. Iravani, "Power management strategies for a micro-grid with multiple distributed generation units," *IEEE Transactions on Power Systems*, vol. 21, no. 4, pp. 1821–1831, 2006.
- [3] M. E. Baran and F. F. Wu, "Optimal sizing of capacitors placed on a radial distribution system," *IEEE Trans. on Power Delivery*, vol. 4, no. 1, pp. 735–743, Jan. 1989.
- [4] K. Turitsyn, P. Šulc, S. Backhaus, and M. Chertkov, "Options for control of reactive power by distributed photovoltaic generators," *Proc. IEEE*, vol. 99, no. 6, pp. 1063–1073, Jun. 2011.
- [5] M. Juamperez, Y. Guangya, and S. B. Kjær, "Voltage regulation in lv grids by coordinated volt-var control strategies," *Journal of Modern Power Systems and Clean Energy*, vol. 2, no. 4, pp. 319–328, 2014.
- [6] J. Smith, W. Sunderman, R. Dugan, and B. Seal, "Smart inverter volt/var control functions for high penetration of pv on distribution systems," in *Power Systems Conference and Exposition (PSCE), 2011 IEEE/PES. IEEE*, 2011, pp. 1–6.
- [7] S. Kundu, S. Backhaus, and I. A. Hiskens, "Distributed control of reactive power from photovoltaic inverters," in *Circuits and Systems (ISCAS), 2013 IEEE International Symposium on. IEEE*, 2013.
- [8] N. Li, G. Qu, and M. Dahleh, "Real-time decentralized voltage control in distribution networks," in *52nd Annual Allerton Conference on Communication, Control, and Computing. IEEE*, 2014.
- [9] V. Kekatos, L. Zhang, G. B. Giannakis, and R. Baldick, "Voltage regulation algorithms for multiphase power distribution grids," *IEEE Transactions on Power Systems*, vol. PP, no. 99, 2015.
- [10] M. Farivar, X. Zhou, and L. Chen, "Local voltage control in distribution systems: An incremental control algorithm," *IEEE International Conference on Smart Grid Communications (SmartGridComm)*, 2015.
- [11] M. Farivar, L. Chen, and S. Low, "Equilibrium and dynamics of local voltage control in distribution systems," in *IEEE 52nd Conference on Decision and Control (CDC), 2013. IEEE*, 2013, pp. 4329–4334.
- [12] E. Dell'Anese, H. Zhu, and G. Giannakis, "Distributed optimal power flow for smart microgrids," *submitted to IEEE Transactions on Smart Grid*, 2013, arXiv preprint available [math.OA] 1211.5856.
- [13] J. Lavaei and S. H. Low, "Zero duality gap in optimal power flow problem," *IEEE Trans. Power Syst.*, 2011.
- [14] B. Zhang, A. Lam, A. Dominguez-Garcia, and D. Tse, "An optimal and distributed method for voltage regulation in power distribution systems," *Power Systems, IEEE Transactions on*, vol. PP, no. 99, pp. 1–13, 2014.
- [15] S. Bolognani, R. Carli, G. Cavraro, and S. Zampieri, "Distributed reactive power feedback control for voltage regulation and loss minimization," *IEEE Transactions on Automatic Control*, vol. 60, no. 4, pp. 966–981, April 2015.
- [16] "Ieee draft recommended practice for establishing methods and procedures that provide supplemental support for implementation strategies for expanded use of ieee standard 1547," *IEEE P1547.8/D8*, pp. 1–176, 2014.

- [17] S. Bolognani, R. Carli, G. Cavraro, and S. Zampieri, "A distributed control strategy for optimal reactive power flow with power constraints," in *IEEE Conference on Decision and Control (CDC)*. IEEE, 2013.
- [18] W. H. Kersting, "Radial distribution test feeders," in *IEEE Power Engineering Society Winter Meeting*, vol. 2, Jan. 2001, pp. 908–912.
- [19] R. D. Zimmerman, C. E. Murillo-Sánchez, and R. J. Thomas, "MATPOWER: steady-state operations, planning and analysis tools for power systems research and education," *IEEE Transactions on Power Systems*, vol. 26, no. 1, pp. 12–19, Feb. 2011.
- [20] D. P. Bertsekas and J. N. Tsitsiklis, *Parallel and Distributed Computation: Numerical Methods*. Athena Scientific, 1997.